Ab Initio Embedded Cluster Study of the Adsorption of NH_3 and NH_4^+ in Chabazite

E. H. Teunissen,* A. P. J. Jansen, and R. A. van Santen

Schuit Institute of Catalysis, Theory Group, Eindhoven University of Technology, P.O. Box 513, 5600 MB Eindhoven, The Netherlands

Received: May 20, 1994; In Final Form: November 15, 1994[⊗]

The adsorption of NH_3 in acidic zeolites has been studied extensively experimentally. Therefore, it can be used very well to verify a model used in a quantum chemical calculation. Here, we present a calculation that, from a quantum chemical point of view, should give a reliable description of the adsorption process. We studied the adsorption of NH_3 and NH_4^+ in chabazite with the embedded cluster method using a reasonable basis set, applying the counterpoise correction and including electron correlation. The geometry was partially optimized. With this calculation we verified the reliability of our model and obtained information that cannot be obtained experimentally. The adsorption energies of hydrogen-bonding NH_3 and of NH_4^+ were -70 ± 10 kJ/mol and -120 ± 15 kJ/mol, respectively. The latter value compares very well with the experimental heat of adsorption. NH_4^+ has a high coordination with the zeolite wall; this is confirmed experimentally. A good geometry is obtained if the boundary of the embedded cluster is kept fixed to that of the zeolite crystal.

Introduction

Zeolites are important solid acid catalysts.[1] They are built from SiO_4 and AlO_4^- tetrahedrons linked together such that the crystal structure consists of a three-dimensional system of intersecting channels of molecular dimensions.[2] The characteristic acidic site, the HOSiAl group, is the most important functional group in zeolite catalysis. Therefore, adsorption of NH_3 onto this group and the proton transfer forming NH_4^+ have been studied widely as a probe for acidity. As a result of the abundant experimental information, these adsorption and proton transfer processes have been used to verify the model representing the zeolite and the quantum chemical method. On the other hand, a quantum chemical calculation should also be consistent from a quantum chemical point of view and requires a correct model to represent the zeolite.[3−10]

Concerning the quantum chemical method, we find that a relatively large basis set should be used. It is also important to apply the counterpoise correction (CPC) to correct for the basis set superposition error (BSSE).[11,12] Furthermore, it is important to include electron correlation. A factor as important as the choice of the basis set is the optimization of the geometry to allow relaxation of the lattice after adsorption has taken place.

Concerning the model representing the zeolite, we find that small clusters do not provide a good model for the zeolite acidic site because they show boundary errors.[5] As a result of the saturation of the dangling bonds with hydrogen atoms, the atoms of the boundary of the cluster are in a chemical environment different from that of the crystal and thus behave differently toward the adsorbate. Furthermore, the long-range electrostatic forces of the crystal are nonnegligible.[5] On the other hand, also periodic Hartree−Fock calculations on zeolites,[5,13,14] although providing useful information, cannot be used to describe adsorption processes. Although the model representing the zeolite is better, the quantum chemical methods that can be applied do not give a satisfactory description of the adsorption processes, and geometry optimization is elaborate.

In order to combine the computational advantages of the cluster with the good model offered by the crystal, we developed the embedded cluster method.[15] In this model the zeolite crystal is represented by a zeolite cluster embedded in a correction potential. This potential is the long-range electrostatic potential of the crystal minus the electrostatic potential of the boundary of the cluster. To calculate the wave function of the crystal and the correction potential, we used the CRYSTAL program.[16−20] For a cluster having the boundary errors relatively far from the adsorption site, the embedded cluster method reproduces the adsorption energies from the crystal within a few kilojoules per mole.[15]

The present paper has three aims. The first one is to test whether the embedding method,[15] in combination with a reasonable basis set, the counterpoise correction,[11,12] and electron correlation, is a reliable method to calculate adsorption energies of small molecules in zeolites. The second aim is to study the effect of the different strategies to optimize the geometry on the zeolite and the adsorbate. The geometry of the cluster and the adsorbate is optimized partially, keeping the geometry of the boundary fixed to the geometry of the zeolite crystal, and different orientations of NH_4^+ toward the lattice have been studied. Finally, we would like to obtain information about the position of NH_4^+ and its relative stability. We studied the effect of the deficiencies in the calculation, for example the basis set and the limited geometry optimization, on small clusters. From these comparisons we corrected the calculated heats of adsorption.

Survey of Experimental Data

Experimentally, most information concerning the adsorption of NH_3 in acidic zeolites is obtained from temperature-programmed desorption (TPD), microcalorimetry (MC), X-ray diffraction (XRD), NMR, and infrared measurements. TPD and MC are used to measure the heat of adsorption of NH_3 on the Brønsted acidic site. Although, in principle, TPD measures the activation barrier for the desorption, this quantity is often interpreted as the heat of adsorption. We collected 31 heats of desorption, measured with TPD, on various acidic zeolites: Y, ZSM-5, mordenite, and ferrierite, all of them with various Si/Al ratios.[21−31] The average heat of adsorption on the Brønsted acid site was 129 kJ/mol with a standard deviation of 20 kJ/

[⊗] Abstract published in *Advance ACS Abstracts,* January 15, 1995.

0022-3654/95/2099-1873$09.00/0

mol. We collected 131 heats of adsorption, measured with MC, on various acidic zeolites: Y, ZSM-5, ZSM-11, ferrierite, and mordenite, with various Si/Al ratios.[28-49] The average heat of adsorption was 150 kJ/mol with a standard deviation of 35 kJ/mol. The heat of adsorption seems relatively independent of the structure and the Si/Al ratio of the zeolite and thus seems largely determined by the acidic site itself. Thus, it can serve as a guide for the adequacy of the quantum chemical model.

From NMR measurements some research groups concluded that, in acidic zeolites at low loadings and at room temperature, NH_3 is present in the form of NH_4^+.[50,51] Also the position and the motion of the NH_4^+ ions in the zeolite have been investigated.[52,53] At 77 K the NH_4^+ cations, distorted from their T_d symmetry as a result of the interaction with the zeolite framework, are rotating in the vicinity of the Al tetrahedrons. Infrared measurements of the lattice vibrations of zeolites confirm the NMR measurements in the sense that NH_4^+, instead of NH_3, is the stable species. The lattice vibrations of the Na form and the NH_4^+ form of zeolite Y are almost equivalent whereas the H-form of zeolite Y is different.[54-57]

XRD provides information about the structure and geometry of a crystal. It is very difficult to obtain information about the local geometry around the acidic site, since XRD gives lattice constants and fractional coordinates averaged over the crystal. Silicon and aluminum atomic X-ray scattering factors are too close to each other to allow easy detection of the location of the Brøsted site. Due to both static disorder of the position of the Brøsted site and the difficulty of measuring the H-atom electron density in XRD experiments, no fine details of the local geometry of the acidic site are known. However, average changes in the lattice as a result of the adsorption of NH_3 can be monitored. Experiments on the D form and the ND_4^+ form of zeolite ϱ show that T−O distances (a T atom is a silicon or aluminum atom) and O−T−O and T−O−T angles change upon adsorption of NH_3.[58-60] Apparently, the lattice adjusts itself to the adsorbate, but no details can be obtained. McCusker showed that NH_4^+ is close to two oxygen atoms.[58]

Structure of the Zeolite Crystal and Clusters

We studied the adsorption of NH_3 and NH_4^+ in the acidic form of chabazite. We chose this zeolite because of its small unit cell, making it feasible to perform *ab initio* calculations, and because we could compare the present results with previous calculations.[5,6,15] Chabazite has channels built from eight-rings, rings containing eight tetrahedrons, in three directions, mutually almost perpendicular to each other.[2] NH_3 and NH_4^+ are adsorbed in these channels that have a diameter of 3.8 Å. The chabazite had a Si/Al ratio of 3, the space group is $R3$. The geometry of the chabazite was optimized using the shell model,[61,62] using the parameter set derived by Schröder *et al.*[63] The structure of the chabazite crystal with NH_4^+ adsorbed in it is shown in Figure 1. More detailed information on chabazite and its geometry can be found in ref 5.

The cluster embedded in the chabazite crystal on which NH_3 and NH_4^+ are adsorbed is shown in Figure 2a. The cluster is cut from the crystal; it contains the acidic HOSiAl-group, the oxygen atoms bonded to this group, and the second shell of silicon and aluminum atoms around the acidic site. Two pairs of these silicon atoms are connected with an oxygen atom to form two four-rings. The dangling bonds are saturated with hydrogen atoms put in the direction of the bonds they are saturating, with Si−H and Al−H bond lengths of 1.49 Å. The positions of the atoms of the cluster, except of course for the dangling bond hydrogens, are taken from the crystal. More detailed information on the cluster can be found in ref 5.

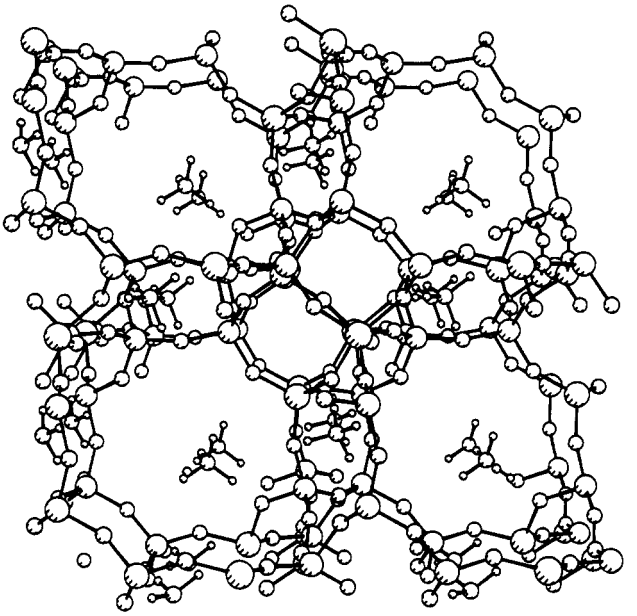

Figure 1. Structure of chabazite with NH_4^+. The view is perpendicular to the one of the eight-ring channels.

Methods and Computational Details

Embedded Cluster Method. The chabazite is described with the embedded cluster method.[15] A cluster is embedded in a crystal by imposing a correction potential. This potential adds the long-range electrostatic potential of the chabazite crystal and subtracts the electrostatic potential of the boundary of the cluster. The correction potential is calculated from the RHF (restricted Hartree−Fock) wave function of the crystal and the cluster. The wave functions of the crystal and the cluster are calculated with the CRYSTAL program,[16-20] using the STO-3G basis set.[64] The correction potential is only added to the atoms of the central $HOSiAlO_6$ group of the cluster. There is a correction for the boundary errors of all the atoms in the cluster, except for those of the central $HOSiAlO_6$ group. We have shown before that, with this cluster, the embedded cluster method reproduces the adsorption energies of the corresponding zeolite crystal with a few kilojoules per mole.[15]

Optimization of the Geometry. The zeolite lattice is flexible and can adjust itself to the presence of an adsorbate. To allow for relaxation of the lattice, the geometry should be optimized. As the atoms are restricted by the zeolite lattice, we have chosen to keep the geometry of the boundary of the cluster fixed to that of the crystal and to optimize only the positions of the atoms close to the adsorbate. In this way, structural features of the chabazite are maintained in the isolated cluster, ensuring good similarity between the acidic site in the crystal and that in the cluster.

The result of such partial optimization depends on the group of atoms that is optimized. To estimate this dependence, we compared the results of the optimization of two different groups of atoms, groups A and B. In group A, we optimized the positions of the atoms of the adsorbate, of the acidic OH group, of the aluminum atom bonded to it, and of the oxygen atoms bonded to the aluminum atom (Figure 3). In group B, the positions of the atoms of the adsorbate and of the atoms of the acidic HOSiAl group were optimized. As another estimate for the effect of the restriction imposed on the cluster by the lattice we compared the adsorption energies of NH_3 on a completely optimized $Al(OH)_3H$ cluster and the same cluster in which the geometry of the AlO_3 group is kept fixed to that found with the corresponding optimization of group A.

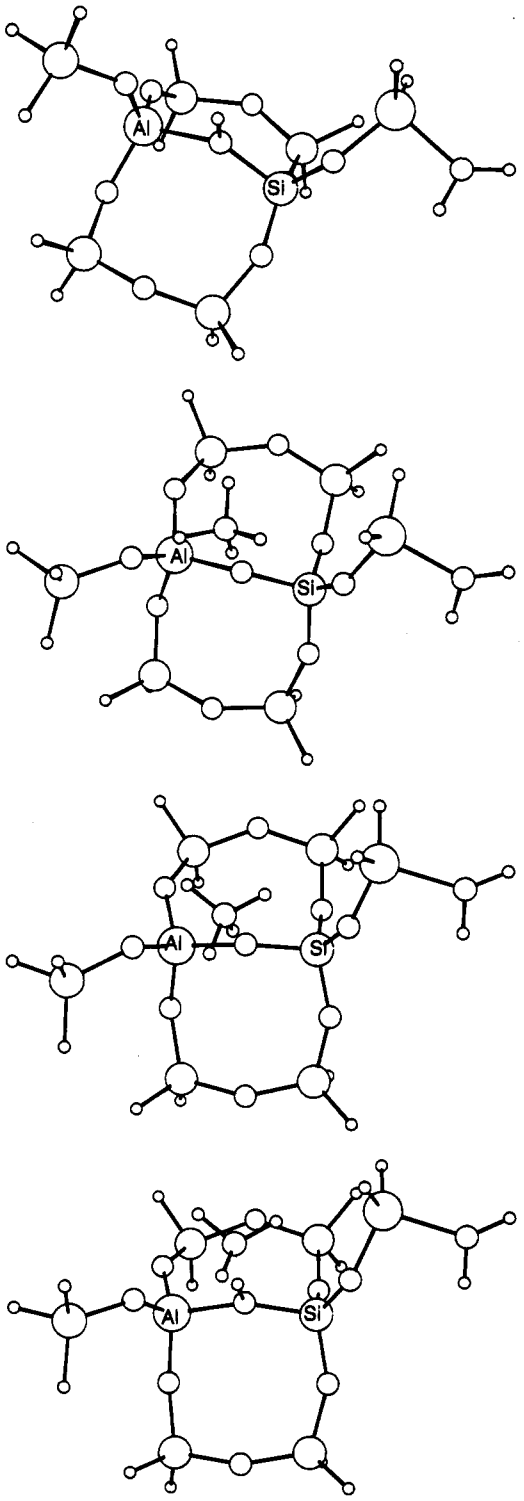

Figure 2. Optimized structures: (A, top) A0; (B, second from top) AI; (C, third from top) AII; (D, bottom) AIII. The Cartesian coordinates of the optimized geometries are available as supplementary material.

We tried to find the geometry corresponding to the minimum in the potential energy surface with optimizations at the RHF level. We followed two different strategies, for both A and B we optimized the cluster without the adsorbate, the A0 and B0 structures. Then, for group A, we optimized NH_4^+ bonding with three hydrogen bonds toward the oxygen atoms of the AlO_4^- tetrahedron, AI. This structure was found favorable in small cluster calculations.[4] To keep NH_4^+ bonded to the zeolite with three hydrogen bonds, the N−H bond lengths were kept fixed at the experimental bond length of 1.03 Å[65] and three dihedral angles H−N−Al−O, determining the coordination of

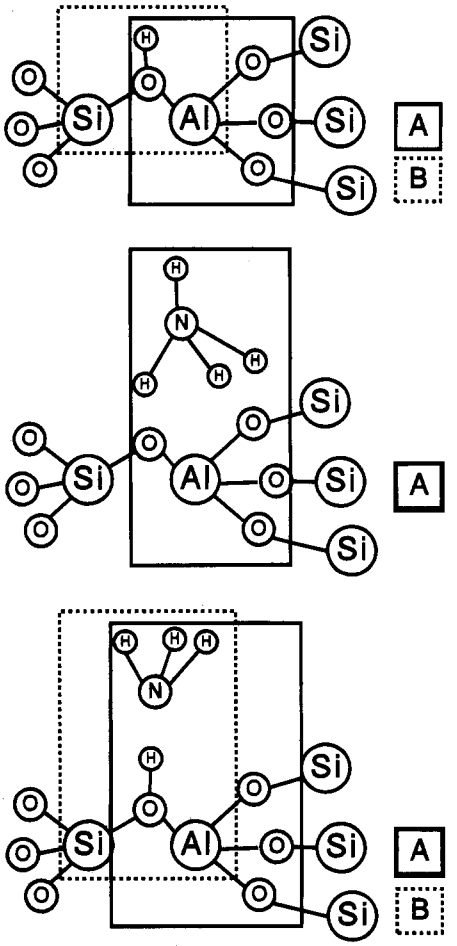

Figure 3. Various strategies to optimize the cluster and the adsorbate. For group A the atoms of the AlO_3 group, the adsorbate, and the acidic proton are optimized. For group B the atoms of the HOSiAl group and the adsorbate are optimized. For both A and B the OH form of the cluster, A0 and B0, is optimized (top). For AI NH_4^+ was optimized keeping the N−H distances and the N−H−O−Al dihedral angle fixed; for AII only the N−H distance of the proton close to the bridging oxygen was kept fixed (middle). For AIII and BIII the positions of the atoms of the respective groups were optimized without further constraints (bottom).

NH_4^+ toward the zeolite lattice, were kept fixed at zero. Starting from this structure, a second one was generated by reoptimizing it with the dihedral angles no longer fixed and by fixing only one N−H distance at 1.03 Å, AII. Finally, a third structure was generated from the second one without any constraints on the adsorbate, AIII. For group B only one optimization, without any constraint on the adsorbate, was carried out, BIII. The different strategies for the optimization are shown in Figure 3.

Calculation of the Adsorption Energy. We calculated the adsorption energies of NH_3 for the structures of groups A and B. As these structures are optimized at the RHF level, they are probably not a minimum in the potential energy surfaces at other levels. Therefore, four extra points for an intermolecular potential energy curve were generated by taking two distances longer and two distance shorter than the equilibrium intermolecular distance at the RHF level. The distance selected as an appropriate intermolecular distance for the potential energy curve depends on the coordination of the adsorbate. We choose the Al···N distance for the AI structure and the O−N distance in the AII, AIII, and BIII structures. These choices are analogous to those in the small cluster calculations.[3,4] The intermolecular potential energy curve is calculated at a correlated level, applying the CPC and embedding the cluster. The

TABLE 1: Some Geometrical Parameters of the A0, AI, AII, AIII, B0, and BIII Structures[a]

parameter	A0	AI	AII	AIII	B0	BIII
r_{O-H}	0.96	1.49	1.50	1.00	0.95	1.00
r_{O-H}		2.24	2.45	2.74		2.76
r_{O-H}		3.77	2.62	3.18		3.35
r_{N-H}	1.00	1.03	1.03	1.01		1.01
r_{N-H}	1.00	1.03	1.02	1.01		1.00
r_{N-H}	1.00	1.03	1.01	1.01		1.00
r_{N-H}		1.03	1.01			
r_{O-Al}	1.87	1.77	1.77	1.84	1.91	1.88
r_{O-Si}	1.68	1.62	1.61	1.67	1.70	1.67
∠Al−O−N		102	107	112		112
∠H−N−H	114	112	110	111		112
∠H−N−H	114	105	108	113		110
∠H−N−H	114	105	104	114		112
∠Si−O−Al	139	141	140	137	136	136
∠N−H−Al−O		0	34	34*		20*
∠N−H−Al−O		0	47	82*		40*
∠N−H−Al−O		0	8	155*		80*

[a] The O−H distances that are tabulated are those between the oxygen atoms of the cluster and the protons of the adsorbate. The three shortest are tabulated. For AIII and BIII the torsion angle H−N−O−Al instead of the torsion angle N−H−Al−O is tabulated; these angles are indicated with an asterisk. The N−H distances and H−N−H angles in the column for A0 refer to the parameters of the free NH_3 molecule.

electron correlation is calculated with second-order Møller−Plesset perturbation theory.[66]

For the geometry optimization as well as for the calculation of the interaction energies, we used the following basis set: the silicon and aluminum atoms have a 6-31G(d) basis set;[67,68] the oxygen atom of the acidic group has a 6-311G(d) basis set;[69] all other oxygen atoms and the nitrogen atom have a 6-31G basis set;[70,71] the acidic proton and the protons of the adsorbate have a 3-1G basis set.[72] All other atoms have a standard minimal STO-3G basis set.[64] This mixed basis set yields the adsorption energy of NH_3 with an error of 10 kJ/mol and underestimates the adsorption energy of NH_4^+ by 40−50 kJ/mol.[3,6,74,75] (Note: the adsorption energies of NH_3 and NH_4^+ on the fixed geometry cluster in ref 3 were repeated at the RHF level with a 6-311++(3df,3dp) basis set.[69,73] At the RHF level the adsorption energies of NH_3 and NH_4^+ were −58 and −15 kJ/mol, respectively. The ΔE_∞^{PT} is 411 kJ/mol at the RHF level and 406 kJ/mol at the MP2 level.)

Results and Discussion

Geometries. The results of the partial geometry optimizations for group A are shown in Figure 3, and some of the geometrical parameters of the optimized structures are given in Table 1. In the AI structure, NH_4^+ was kept triply bonded to the oxygen atoms of the AlO_4^- tetrahedron of the zeolite lattice by keeping the N−H−O−Al dihedral angles fixed at 0°. Previously, we optimized NH_4^+ bonded onto a $Al(OH)_3H^-$ cluster with the same restriction.[4] In the chabazite the coordination is not as regular as the coordination between NH_4^+ and the $Al(OH)_3H^-$ cluster; in the small cluster the distances between the oxygen atoms of the lattice and the proton of the adsorbate were 1.85 Å; in the AI structure the bond lengths vary between 1.49 and 3.77 Å. In the small cluster the interaction between the cluster and NH_4^+ is enlarged by directing the oxygen atoms toward NH_4^+. In the chabazite the atoms are more restricted in their movement because the positions of the atoms in the boundary of the cluster are kept fixed to those in the crystal. NH_4^+ is less stable with respect to the small cluster calculations because the coordination between NH_4^+ and the zeolite in the chabazite is not as high as in the small cluster calculations. In small cluster calculations, where the geometry is fully optimized and where the coordination between the cluster and the adsorbate is crucial,[4,76−82] one should note that the flexibility of the zeolite and thus the stability of the adsorbate are overestimated. The result of the further optimization of the AI structure, without constraints on the dihedral angles determining the coordination, is the AII structure. In the AII structure, with respect to the AI structure, NH_4^+ is rotated around the NO axis, the axis between the nitrogen atom of the adsorbate and the oxygen atom to which the proton was bonded originally.

The result of reoptimization of the AII structure, without any constraints on the adsorbate, is a structure in which the proton has been transferred to the zeolite and NH_3 is hydrogen bonding to the zeolite OH group, the AIII structure. Also the optimization of group B resulted in a hydrogen-bonding NH_3. At the RHF level NH_4^+ is not stable. This is in contrast to our earlier findings that, if NH_4^+ can coordinate to more oxygen atoms in the zeolite, it is favorable over hydrogen-bonding NH_3.[4] NH_4^+ can be unstable because of the absence of diffuse functions on the oxygen atoms in the basis set used here or because of the decreased interaction between the zeolite and NH_4^+ with respect to the small zeolite clusters.

Effect of the Restrictions in the Partial Optimization. We partially optimized the cluster. With this partial optimization the zeolite may appear too rigid. We made an estimate of the adsorption energy that could be gained by a more extended geometry optimization by repeating the optimization of NH_4^+ on the $Al(OH)_3H^-$ cluster, keeping the AlO_3 part fixed to that of the AI structure and comparing the adsorption energy to that of the fully optimized $Al(OH)_3H^-$ cluster. Because of the less optimal coordination in the structure in which the AlO_3 part is kept fixed, the adsorption energy of NH_4^+ is 29 kJ/mol less at the RHF level. The adsorption energy is lower because the oxygen atoms are bonded to the fixed silicon atoms and thus cannot coordinate optimally to the adsorbate.

In a more extended optimization the coordination may be improved because the silicon atoms, linked to the oxygen atoms of the AlO_4 tetrahedron, can be displaced. The extra interaction that can be gained maximally by the displacement of the silicon atoms in a more extended geometry optimization is 29 kJ/mol. This value is an upper bound because, first, by increasing the interaction with the aluminum tetrahedron the interaction with the other parts of the zeolite is decreased and, second, in order to increase the interaction, the zeolite lattice has to be deformed. The deformation energy has to be subtracted from the interaction energy that is gained.

We made a rough estimate of the deformation energy required to obtain optimal coordination between the NH_4^+ and the zeolite lattice. The deformation energy, caused by the displacement of the silicon atoms to accommodate the deformed tetrahedron, is roughly estimated from the deformation of small clusters. We estimated the deformation of the Al−O and Si−O stretching and for the Al−O−Si bending on a $OSiAlH_6^-$ cluster and the Si−O−Si bending on a OSi_2H_6 cluster. The stretching of the Al−O and Si−O bonds by 0.05 Å, necessary for the optimal configuration, cost 2.1 and 5.7 kJ/mol, respectively. The bending of the angles by 10° cost 1.7 and 0.8 kJ/mol, respectively. Thus, it seems more favorable to displace the silicon atoms by the bending of the Si−O−Al and Si−O−Si angles, although some stretching will also appear. For each displaced silicon atom, two Si−O−Si angles and one Si−O−Al angle must be bent. The displacement of one silicon atom costs 4 kJ/mol, and thus, the displacement of three silicon atoms will cost 12 kJ/mol. Thus, in this simple model, not including the stretching of bonds, apart from those in the AlO_3 part, the deformation energy is 12 kJ/mol.

The adsorption energy that can maximally be gained by a more extended geometry optimization is 17 kJ/mol.[12-29] From this number we should also subtract the decrease in interaction between NH_4^+ and the other atoms in the eight-ring, as a result of the higher coordination to the aluminum tetrahedron, and the deformation energy, as a result of the stretching of the bonds not taken into account in the simple model to calculate adsorption energies. This means the adsorption energy that can be gained maximally by a more extended optimization is 10-15 kJ/mol.

Validity of the Partial Optimization. Another estimate for the effect of the partial, instead of a full, optimization can be made from the differences between the adsorption energies of NH_3 for groups A and B. In group A the $HOAlO_3$ group was optimized, and in group B the HOSiAl group was. The difference in the adsorption energy of NH_3 is 10 kJ/mol at the RHF level. This is a relatively large difference and the partial optimization does not seem valid, but we should keep in mind that one of the differences between group A and group B is the optimization of the position of the silicon atom, an atom close to the adsorbate in the hydrogen-bonded structure. The effect of further enlargement of the group of atoms to be optimized will be less than 10 kJ/mol. In principle, the adsorption energy of NH_4^+ is more dependent on the geometry. However, an enlargement of the group of atoms that are optimized, for example in the AI structure, will not have a large effect on the adsorption energy. Already all the atoms close to NH_4^+ are optimized. An estimate of the effect of a more extended optimization is 10 kJ/mol.

The deformations we find with the optimization are similar to those found experimentally. For example, there is a difference in cell constants and average T-O bond lengths of 1 or 2% between the H form and the NH_4^+ form of zeolite ϱ.[58,59] These numbers are consistent with the deformations we found. Although the geometry optimization presented here slightly underestimates the adsorption energy, the partial optimization seems to be the right strategy to obtain the proper geometry.

Basis Set Effects. The basis set in this paper is relatively small and will give an error in the calculated adsorption energies. To obtain an estimate for this error, we repeated the calculations of NH_4^+ triply coordinated on a $Al(OH)_3H^-$ cluster as in ref 4 with the basis set used in this paper. The geometries of the $NH_4^+\cdots Al(OH)_3H^-$ complex and the $Al(OH)_3H_2$ cluster were fully geometry optimized. The N-H distances and the dihedral angles H-N-Al-O, determining the coordination, were kept fixed. The adsorption energy at the MP2/CPC level with the basis set used here was -85 kJ/mol, about 30 kJ/mol less than with the larger basis set.[4] This larger basis set itself underestimates the stability of NH_4^+ by 10-15 kJ/mol.

Calculation of the Adsorption Energies. The adsorption energies of NH_3 and NH_4^+ for the various structures are tabulated in Table 2. The most accurate adsorption energies are those including electron correlation, the CPC, and the long-range electrostatic forces of the crystal. These calculations are denoted MP2/CPC/EMB. At this level, the adsorption energies of NH_3 in the AI and the AIII structure NH_4^+ are almost equal. The effect of the CPC is much larger than in the small cluster calculations.[3,4] Already at the RHF level it is very large, and at the MP2 level the largest part of the interaction energy appears to be BSSE. The BSSE is larger than in the small cluster calculations[3,4] for two reasons. First, the basis set is smaller than in the small cluster calculations. On comparing different basis sets on the small clusters we saw that a smaller basis set increases the BSSE.[3] Second, the cluster is much larger. Thus, there are more atoms providing orbitals that can be used by the interacting particles, the adsorbate, and the zeolite cluster, to lower their energy, in this way increasing the BSSE.[11,12] From the magnitude of the BSSE we conclude that adsorption energies for systems as described here must be calculated with the use of the CPC.

TABLE 2: Adsorption Energies of NH_3 and NH_4^+, for AI, AII, AIII, and BIII[a]

	AI		AII		AIII		BIII	
method	ΔE	R_{NO}	ΔE	R_{NO}	ΔE	R_{AlN}	ΔE	R_{NO}
RHF	-31	3.31	-38	2.52	-77	2.72	-87	2.68
RHF/CPC	-5	3.52	6	2.55	-31	2.80	-41	2.76
MP2	-67	3.32	-69	2.52	-98	2.68		
MP2/CPC	-36	2.80	-9	2.56	-26	3.53		
RHF/EMB	-48	3.31	-64	2.55	-92	2.71	-99	2.67
RHF/CPC/EMB	-28	3.55	-21	2.59	-45	2.77	-52	2.74
MP2/EMB	-84	3.32	-94	2.55	-113	2.66		
MP2/CPC/EMB	-50	3.55	-36	2.60	-51	2.78		

[a] The adsorption energies are calculated at the RHF level and at the MP2 level, with and without the CPC, and for the embedded cluster (EMB) and for the nonembedded cluster. The adsorption energies are in kJ/mol, and intermolecular distances are in Å.

The effect of the electron correlation, if the CPC is applied, is comparable to that in the small cluster calculations.[3,4] Electron correlation stabilizes NH_4^+ because it stabilizes the anionic lattice. It stabilizes both NH_3 and NH_4^+ because a part of the Van der Waals energy is included. With the cluster and this basis set, not all the Van der Waals interaction energy between the zeolite and the adsorbate is obtained. From the adsorption energy of CH_4, having the same number of electrons as NH_3 and NH_4^+ in zeolite X,[83] the missing Van der Waals energy is estimated to be 10 kJ/mol. The effect of the embedding is almost the same as found in earlier calculations, in which the geometries of the cluster and the adsorbate were not optimized.[6,15]

We can question the value of the geometry optimizations at the RHF level. As the geometry is optimized at a level that underestimates the stability of NH_4^+, constraints must be used to avoid proton transfer from NH_4^+ to the zeolite. The effect of the constraints on the geometry and the interaction energy is relatively small, because the main part of the effect of the optimization on the adsorption energy lies in the relaxation of the lattice and not in the deformation of NH_4^+. A larger problem of the RHF optimization is that the potential energy surface may be quite different from that of the MP2/CPC/EMB level. The effect of the embedding on the optimization is negligible; the internal geometry of the lattice and the adsorbate cluster distances are almost independent of the embedding.[6,15] The effect of the BSSE in the optimizations is large: at the RHF level AII is more stable than AI. This stability however is to a large degree the result of an increase in the BSSE: after the CPC, AI appears to be more stable than AII.

We tried to avoid the shortcomings of the optimization at the RHF level by calculating the interaction from an appropriate potential energy curve. Even so, the optimization of the geometry at the RHF level will certainly cause some errors in the geometry and the adsorption energy. It is difficult to give an estimate for the error in the adsorption energies caused by the optimization of the geometry at the RHF level; it will however not be much larger than 10 kJ/mol.

Comparison between the Experimental and Calculated Adsorption Energies. It is only possible to make a comparison between the calculated adsorption energies and the experimental heats of adsorption if we make a correction for the deficiencies and the errors in the calculation. The largest deficiency is the limited size of the basis set; it does not have a large effect on

the adsorption energy of NH_3,[3] but the adsorption energy of NH_4^+ is underestimated by 40−50 kJ/mol. Other errors are caused by the limited geometry optimization, the optimization at the RHF level, and the error in the calculation of the Van der Waals energy. If we take into account the errors and the deficiencies of the calculation, the adsorption energy of NH_3 will be about -70 ± 10 kJ/mol. The adsorption energy of NH_4^+, in the favorable AI structure, will be about -120 ± 15 kJ/mol. The latter compares quite well with the experimental heat of adsorption of -129 ± 20 kJ/mol measured with TPD and -150 ± 35 kJ/mol measured with MC.

Conclusion

We performed a quantum chemical study on the adsorption of NH_3 and NH_4^+ in acidic chabazite. The calculations were performed with the embedded cluster method using a reasonable basis set, including electron correlation and applying the counterpoise procedure. The geometry of the adsorbate, and the part of the cluster interacting with it, was optimized. The boundary of the cluster was kept fixed.

The adsorption energies of NH_3 and NH_4^+, the latter in a conformation with a high coordination toward the zeolite lattice, are almost equivalent: −51 and −50 kJ/mol, respectively. If the calculated adsorption energies are corrected for their errors, such as the deficiencies in the basis set, the incomplete Van der Waals energy, the partial optimization, and the errors made with the optimization at the RHF level, the adsorption energies are -70 ± 10 kJ/mol and 120 ± 15 kJ/mol, respectively. The latter value compares quite well with the experimental heat of adsorption. This means that we developed a reliable method to calculate adsorption energies of small molecules in zeolites. Second, the best way to obtain the geometry of the zeolite and the adsorbate is to optimize the geometry partially. Third, from the results we can confirm the experimental findings that the adsorbate is present in the form of NH_4^+, having a high coordination with the zeolite lattice.

Acknowledgment. We acknowledge support from the EC (Contract No. SC 1000199). The computer time on the Cray Y-MP4/464 was subsidized by the National Computing Facilities (NCF) Foundation (Grant SC-183).

Supplementary Material Available: The geometries of the crystal and the optimized structures (A0, AI, AII, AIII, B0, BIII) (7 pages). Ordering information is available on any current masthead page.

References and Notes

(1) van Bekkum, H.; Flanigen, E. M.; Jansen, J. C. *Introduction to zeolite science and practice*; Elsevier: Amsterdam, 1991.
(2) Meier, W. M.; Olson, D. H. *Atlas of Zeolite Structure Types*, 2nd ed.; Butterworths: London, 1987.
(3) Teunissen, E. H.; van Duijneveldt, F. B.; van Santen, R. A. *J. Phys. Chem.* **1992**, *96*, 366.
(4) Teunissen, E. H.; van Santen, R. A.; Jansen, A. P. J.; van Duijneveldt, F. B. *J. Phys. Chem.* **1993**, *97*, 203.
(5) Teunissen, E. H.; Roetti, C.; Pisani, C.; de Man, A. J. M.; Jansen, A. J. P.; Orlando, R.; van Santen, R. A.; Dovesi, R. *Mod. Simul. Mater. Sci. Eng.* **1994**, 921.
(6) Teunissen, E. H.; Jansen, A. P. J. *Int. J. Quantum Chem.*, in press.
(7) Sauer, J.; Horn, H.; Häser, M.; Ahlrichs, R. *Chem. Phys. Lett.* **1990**, *173*, 26.
(8) Sauer, J.; Kölmel, C. M.; Hill, J.-R.; Ahlrichs, R. *Chem. Phys. Lett.* **1989**, *164*, 193.
(9) Brand, H. V.; Curtiss, L. A.; Iton, L. E. *J. Phys. Chem.* **1992**, *96*, 7725.
(10) Brand, H. V.; Curtiss, L. A.; Iton, L. E. *J. Phys. Chem.* **1993**, *97*, 12773.
(11) Boys, S. F.; Bernardi, F. B. *Mol. Phys.* **1970**, *19*, 553.
(12) van Lenthe, J. H.; van Duijneveldt-van de Rijdt, J. G. C. M.; van Duijneveldt, F. B. *Adv. Chem. Phys.* **1987**, *79*, 521.
(13) White, J. C.; Hess, A. C. *J. Phys. Chem.* **1993**, *97*, 6398.
(14) White, J. C.; Hess, A. C. *J. Phys. Chem.* **1993**, *97*, 8703.
(15) Teunissen, E. H.; Jansen, A. P. J.; van Santen, R. A.; Orlando, R.; Dovesi, R. *J. Chem. Phys.* **1994**, *101*, 5865.
(16) Pisani, C.; Dovesi, R.; Roetti, C. *Hartree−Fock Ab−initio Treatment of Crystalline Systems, Lecture Notes in Chemistry*; Springer Verlag: Berlin, 1988; Vol. 48.
(17) Pisani, C.; Dovesi, R. *Int. J. Quantum Chem.* **1980**, *17*, 501.
(18) Dovesi, R.; Pisani, C.; Roetti, C.; Saunders, V. R. *Phys. Rev. B* **1983**, *28*, 5781.
(19) Dovesi, R. *Int. J. Quantum Chem.* **1986**, *29*, 1755.
(20) Dovesi, R.; Saunders, V. R.; Roetti, C. *Crystal 92 Users's Manual*; Gruppo di Chimica Teorica, Università di Torino, and SERC Laboratory: 1992.
(21) Topsøe, N.-Y.; Pedersen, K.; Derouane, E. G. *J. Catal.* **1981**, *70*, 41.
(22) Dima, E.; Rees, L. V. C. *Zeolites* **1987**, *10*, 8.
(23) Hidalgo, C. V.; Itoh, H.; Hattori, T.; Niwa, M.; Murakumi, Y. *J. Catal.* **1984**, *85*, 362.
(24) Karge, H. G.; Dondur, V. *J. Phys. Chem.* **1990**, *94*, 765.
(25) Karge, H. G.; Dondur, V.; Weitkamp, J. *J. Phys. Chem.* **1991**, *95*, 283.
(26) Post, J. G.; van Hooff, J. H. C. *Zeolites* **1984**, *4*, 9.
(27) Bankós, I.; Valyon, J.; Kapustin, G. I.; Kalló, D.; Klyachko, A. L.; Brueva, T. R. *Zeolites* **1988**, *8*, 189.
(28) Karge, H. G. *Stud. Surf. Sci. Catal.* **1991**, *65*, 133.
(29) Sawa, M.; Niwa, M.; Murakumi, Y. *Zeolites* **1990**, *10*, 307.
(30) Kapustin, G. I.; Brueva, T. R.; Klyachko, A. L.; Beran, S.; Wichterlová, B. *Appl. Catal.* **1988**, *42*, 239.
(31) Auroux, A.; Jin, Y. S.; Vedrine, J. C.; Benoist, L. *Appl. Catal.* **1988**, *36*, 323.
(32) Auroux, A.; Vedrine, J. C. In *Catalysis by acids and bases*; Imelek, B., Ed.; Elsevier: Amsterdam, 1985.
(33) Auroux, A.; Bolis, V.; Wierzchowski, P.; Gravelle, P. C.; Vedrine, J. C. *J. Chem. Soc., Faraday Trans. 1* **1979**, *75*, 2544.
(34) Shi, Z. C.; Auroux, A.; Taarit, Y. B. *Can. J. Chem.* **1988**, *66*, 1013.
(35) Tsutsumi, K.; Mitani, Y.; Takahashi, H. *Bull. Chem. Soc. Jpn.* **1983**, *56*, 1912.
(36) Mitani, Y.; Tsutsumi, K.; Takahashi, H. *Bull. Chem. Soc. Jpn.* **1983**, *56*, 1917.
(37) Mitani, Y.; Tsutsumi, K.; Takahashi, H. *Bull. Chem. Soc. Jpn.* **1983**, *56*, 1921.
(38) Vedrine, J. C.; Auroux, A.; Bolis, V.; Dejaifve, P.; Nacchane, C.; Wierzchowski, P.; Derouane, E. G.; Nagy, J. B.; Gilson, J.-P.; van Hooff, J. H. C.; van den Berg, J. P.; Wolthuizen, J. *J. Catal.* **1979**, *59*, 248.
(39) Klyachko, A. L.; Kapustin, GH. I.; Brueva, T. R.; Rubinstein, A. M. *Zeolites* **1987**, *7*, 119.
(40) Lohse, U.; Parlitz, B.; Patzelova, V. *J. Phys. Chem.* **1989**, *93*, 3677.
(41) Parillo, D. J.; Gorte, R. J. *J. Phys. Chem.* **1993**, *97*, 8786.
(42) Stach, H.; Jänchen, J.; Jerscekewitz, H.-G.; Lohse, U.; Parlitz, B.; Hunger, M. *J. Phys. Chem.* **1992**, *96*, 8480.
(43) Shannon, R. D.; Gardner, K. H.; Staley, R. H.; Bergeret, G.; Gallezot, P.; Auroux, A. *J. Phys. Chem.* **1985**, *89*, 4778.
(44) Sayed, M. B.; Aline, A.; Vedrine, J. C. *Appl. Catal.* **1986**, *23*, 49.
(45) Spiewak, B. E.; Handy, B. E.; Sharma, S. B.; Dumesic, J. A. *Catal. Lett.* **1994**, *23*, 207.
(46) Cardona-Martinez, N.; Dumesic, J. A. *Adv. Catal.* **1992**, *38*, 149 and references therein.
(47) Vorbeck, G.; Jänchen, J.; Parlitz, B.; Schneider, M.; Fricke, R. *J. Chem. Soc., Chem. Commun.* **1994**, 123.
(48) Parillo, D. J.; Gorte, R. J. *J. Phys. Chem.* **1993**, *97*, 8786.
(49) Parillo, D. J.; Lee, C.; Gorte, R. J. *Appl. Catal.* **1994**, *110*, 67.
(50) Earl, W. L.; Fritz, P. D.; Gibson, A. A. V.; Lunsford, J. H. *J. Phys. Chem.* **1987**, *91*, 2091.
(51) Michel, D.; Germanus, A.; Pfeifer, H. *J. Chem. Soc., Faraday Trans. 1* **1982**, *78*, 237.
(52) Vega, A. J.; Luz, Z. *J. Phys. Chem.* **1987**, *91*, 365.
(53) Deininger, D.; Reïman, B. *Z. Phys. Chem. (Leipzig)* **1972**, *251*, 351.
(54) van Santen, R. A.; de Man, A. J. M.; Jacobs, W. P. J. H.; Teunissen, E. H.; Kramer, G. J. *Catal. Lett.* **1991**, *9*, 273.
(55) Stock, T.; Dombrowski, D.; Fruwert, J. *Z. Phys. Chem. (Leipzig)* **1984**, *265*, 738.
(56) Jacobs, W. P. J. H.; van Wolput, J. H. M. C.; van Santen, R. A. *J .Chem. Soc., Faraday Trans.* **1993**, *89*, 1271.
(57) Jacobs, W. P. J. H.; van Wolput, J. H. M. C.; van Santen, R. A. *Zeolites* **1993**, *13*, 170.
(58) McCusker, L. B. *Zeolites* **1984**, *4*, 51.
(59) Corbin, D. R.; Abrams, L.; Jones, G. A.; Eddy, M. M.; Harrison, W. T. A.; Stucky, G. D.; Cox, D. E. *J. Am. Chem. Soc.* **1990**, *112*, 4821.

(60) Fischer, R. X.; Bauer, W. H.; Shannon, R. D.; Parise, J. B.; Faber, J.; Prince, E. *Acta Crystallogr.* **1989**, *C45*, 983.
(61) Dick, B. G.; Overhauser, A. W. *Phys. Rev.* **1958**, *112*, 91.
(62) Catlow, C. R. A.; Dixon, M.; Mackrodt, W. C. *Computer simulation of solids, Lecture Notes in Physics*; Springer: Berlin, 1982; Vol. 166.
(63) Schröder, K.-P.; Sauer, J.; Leslie, M.; Catlow, C. R. A. *Zeolites* **1992**, *12*, 20. Schröder, K.-P.; Sauer, J.; Leslie, M.; Catlow, C. R. A.; Thomas, J. M. *Chem. Phys. Lett.* **1992**, *188*, 320.
(64) Hehre, W. J.; Stewart, R. F.; Pople, J. A. *J. Chem. Phys.* **1969**, *51*, 2657.
(65) Ibers, J. A.; Stevenson, D. P. *J. Chem. Phys.* **1958**, *28*, 929.
(66) Møller, C.; Plesset, M. S. *Phys. Rev.* **1934**, *46*, 618.
(67) Franci, M. M.; Pietro, W. J.; Hehre, W. J.; Binkley, J. J.; Gordon, M. S.; DeFrees, D. J.; Pople, J. A. *J. Chem. Phys.* **1982**, *77*, 3654.
(68) Gordon, M. S.; Binkley, J. S.; Pople, J. A.; Pietro, W. J.; Hehre, W. J. *J. Am. Chem. Soc.* **1982**, *104*, 2797.
(69) Krishnan, R.; Binkley, J. S.; Seeger, R.; Pople, J. A. *J. Chem. Phys.* **1980**, *72*, 650.
(70) Hehre, W. J.; Ditchfield, R.; Pople, J. A. *J. Chem. Phys.* **1972**, *56*, 2257.
(71) Hariharan, P. C.; Pople, J. A. *Theor. Chim. Acta* **1973**, *28*, 213.
(72) Ditchfield, R.; Hehre, W. J.; Pople, J. A. *J. Chem. Phys.* **1971**, *54*, 724.
(73) Frisch, M. J.; Pople, J. A.; Binkley, J. S. *J. Chem. Phys.* **1984**, *80*, 3265.
(74) DeFrees, D. J.; McLean, A. D. *J. Comput. Chem.* **1986**, *7*, 321.
(75) Szalewich, K.; Cole, S. J.; Kolos, W.; Bartlett, R. J. *J. Phys. Chem.* **1988**, *89*, 3662; **1990**, *112*, 4821.
(76) Kassab, E.; Fouquet, J.; Allavena, M.; Evleth, E. M. *J. Phys. Chem.* **1993**, *97*, 9034.
(77) Medin, A. S.; Borovkov, V. Yu.; Kazanksy, V. B.; Pelmenschikov, A. G.; Zhidomirov, G. M. *Zeolites* **1990**, *10*, 668.
(78) Pelmenschikov, A. G.; Morosi, G.; Gamba, A. *J. Phys. Chem.* **1992**, *96*, 2241.
(79) Pelmenschikov, A. G.; van Santen, R. A. *J. Phys. Chem.* **1993**, *97*, 10678.
(80) Pelmenschikov, A. G.; van Santen, R. A.; Jänchen, J.; Meijer, E. L. *J. Phys. Chem.* **1993**, *97*, 11071.
(81) Sierra, L. R.; Kassab, E.; Evleth, E. M. *J. Phys. Chem.* **1993**, *97*, 641.
(82) Senchenya, I. N.; Kazansky, V. B. *Catal. Lett.* **1991**, *8*, 317.
(83) Zhang, S.-Y.; Talu, O.; Hayhurst, D. T. *J. Phys. Chem.* **1991**, *95*, 1722.

JP941238A